ANTINUCLEONS[1]

By Emilio Segrè[2]

Physics Department, University of California, Berkeley, California

Introduction

The idea of "antiparticles," as is well known, originated with Dirac, who in establishing the relativistic equations for the electron noted that besides the solutions corresponding to ordinary electrons there were also "unwanted solutions" corresponding to particles of electronic mass but of charge $+e$ instead of the electronic charge $-e$. (45). The discovery of the positron by Anderson (10) offered a brilliant experimental confirmation of Dirac's prediction and gave the first example of an "antiparticle."

One could think of applying Dirac's theory of the electron without changes, except in the mass of the particle, to the proton; however, this view is obviously untenable because the magnetic moment of the proton is not one nuclear magneton, nor would it account for the neutron which is clearly related to the proton. Even if such a literal extension of Dirac's theory is impossible, the feature of giving sets of solutions which represent "charge-conjugate" particles is preserved in all theories of elementary particles. In particular the appearance of the anomalous moment of the proton is no obstacle because it is ascribed to the pion cloud surrounding it, and the interaction between pions and nucleons is of the "strong" type for which invariance on charge conjugation is valid (105). We shall consider here only fermions of spin $\frac{1}{2}$. For them a particle and its "charge conjugate" are related by the set of properties given in Table I.

Properties 1 to 5, inclusive, are established by very general arguments and require only invariance under the product of charge conjugation C, space reflection P, and time reversal T(CPT theorem); they are rigorously true even if invariance under charge conjugation alone is not valid [see (105)].

Originally, properties 1 to 4 were derived from the principle of invariance under charge conjugation, which can be formulated by saying that a possible physical situation is transformed into another possible physical situation by changing the sign of all electric charges. Since this principle is violated in weak interactions, it is important to point out that it is not necessary to establish the properties listed above, but that the weaker requirement expressed by the invariance under the CPT transformation is sufficient (76, 77).

[1] The survey of the literature pertaining to this review was completed in April, 1958.

[2] The author is indebted to Drs. G. Chew, G. Goldhaber, H. Steiner, and T. Ypsilantis for reading the manuscript and offering very useful comments.

TABLE I

PARTICLE-ANTIPARTICLE RELATIONS

	Particle		Antiparticle
1) Charge	q		$-q$
2) Mass	m		m
3) Spin		same	
4) Magnetic moment	μ		$-\mu$
5) Mean life		same	
6) Creation		in pairs	
7) Annihilation		in pairs	

Properties 6 and 7 in the nuclear case are a consequence of the conservation of nucleons; the number of antinucleons must be subtracted from the number of nucleons in establishing the nucleon number of a system.

VERIFICATION OF DIRAC'S ATTRIBUTES OF THE ANTIPROTON

After the discovery of the positron in cosmic rays it was natural to expect that antinucleons also might be found there; indeed, prior to 1955, processes in which the energies available were sufficient to produce nucleon-antinucleon pairs occurred only in cosmic rays. Several cosmic-ray events (5, 24, 25, 98) have been observed in cloud chambers and in photographic emulsions which are attributable to antiprotons. In none of them, however, is the evidence obtained sufficient to establish with certainty the identity of the particle involved.

With the advent of accelerators powerful enough to produce antinucleons in the laboratory, it became possible to investigate systematically antiprotons and antineutrons, and to identify them beyond any doubt. The first successful investigation was carried on by Chamberlain, Segrè, Wiegand & Ypsilantis with the Berkeley Bevatron in the fall of 1955 (38, 39). Charge, mass, and stability against spontaneous decay of the antiproton were the first properties ascertained.

The central problem was to find particles with charge $-e$ and mass equal to that of the proton. This was accomplished by determining the sign and magnitude of the charge, and the momentum and velocity of the particle. From the relation

$$p = mc\beta\gamma \qquad 1.$$

the mass was then found. Here p is the momentum, m the rest mass, c the velocity of light, v the velocity of the particle, and $\beta = v/c$, $\gamma = (1-\beta^2)^{-1/2}$.

The apparatus employed is shown in Figure 1. The trajectory of the particles fixes their momentum if the charge and the magnetic fields are known. The latter are measured directly and the trajectory is checked by the wire-orbit method: a flexible wire with an electric current i and subject

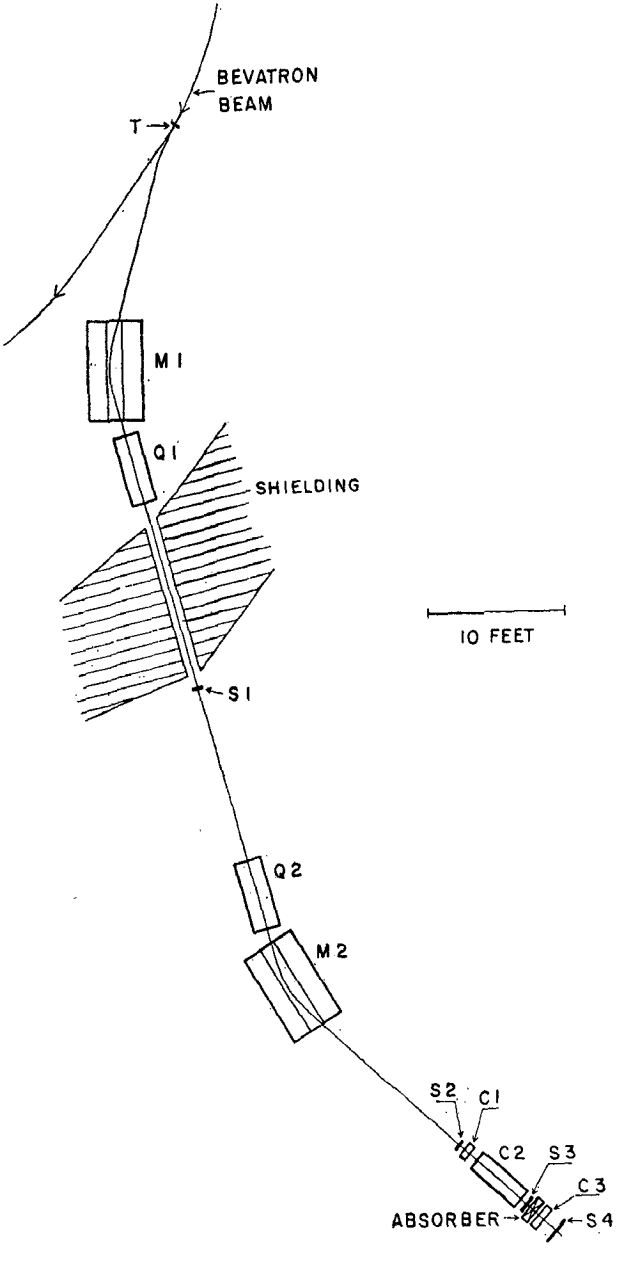

FIG. 1. Original mass spectrograph of Chamberlain, Segrè, Wiegand, & Ypsilantis (39)
For characteristics of components see Table II.

TABLE II

CHARACTERISTICS OF COMPONENTS OF THE APPARATUS

S1, S2	Plastic scintillator counters 2.25 in. diameter by 0.62 in. thick
C1	Cerenkov counter of fluorochemical O-75, ($C_8F_{16}O$); $\mu_D=1.276$; $\rho=1.76$ gm. cm.$^{-3}$ Diameter 3 in.; thickness 2 in.
C2	Cerenkov counter of fused quartz: $\mu_D=1.458$; $\rho=2.2$ gm. cm.$^{-3}$ Diameter 2.38 in.; length 2.5 in.
Q1, Q2	Quadrupole focusing magnets: Focal length 119 in.; aperture 4 in.
M1, M2	Deflecting magnets 60 in. long. Aperture 12 in. by 4 in. B≅13,700 gauss

to a mechanical tension T in the magnetic field takes exactly the form of the orbit of a particle of charge e and momentum p if

$$T/i = p/e. \qquad 2.$$

The particles in passing through the scintillation counters $S_1S_2S_3$ give rise to pulses having the same pulse height as those caused by protons of the same momentum, thus indicating that the magnitude of the charge is e and not $2e$ or greater. The trajectory determines the momentum p and also that the sign of the charge is negative. The measurement of the velocity is the most difficult part of the experiment, especially because antiprotons are accompanied by a very heavy background flux of pions mixed with some electrons and muons in a ratio of the order of 50,000 pions to one antiproton. It is accomplished by measuring the time of flight between scintillators S_1, S_2, and corroborated by the response of the special (40, 106) Cerenkov Counter C_2 which responds only to particles with $0.75<\beta<0.78$. Cerenkov Counter C_1 is in anticoincidence and responds to particles with $\beta>0.79$, helping to eliminate pions and lighter particles. Scintillator S_3 has the purpose of ensuring that the antiproton traverses the whole apparatus.

The momentum of a particle passing through the instrument was 1.19 Bev/c. The velocity of an antiproton of this momentum is $0.78c$, whereas a meson of the same momentum has $v=0.99c$. Their times of flight between S_1 and S_2 were 51 and 40 millimicroseconds, respectively. The time of flight and the response of C_2 represent independent velocity measurements, and combined with the other counters as described allow the identification of the particle as an antiproton and a measurement of its mass to within 5 per cent accuracy. This apparatus delivers at S_3 certified antiprotons, i.e., it ensures that when the expected electronic signals appear, an antiproton has passed through it and emerged at S_3.

A more luminous version of the apparatus which gives about 80 times as many antiprotons as the one described above has also been described (2). At 6.2 Bev this last apparatus gives, as an order of magnitude for practical purposes, one transmitted antiproton of momentum 1.19 Bev/c for every 2×10^{10} protons impinging on a carbon target 6 in. thick.

A spectrograph using repeated time-of-flight measurements, without Cerenkov counters, has been built by Cork and his co-workers (42); its performance is similar to that of the spectrograph in (2), but it is better suited for lower momenta where Cerenkov counters are inconvenient.

The following sections contain discussions of the extent to which the properties mentioned in Table I have been verified.

Charge.—The sign of the charge is determined by the curvature of the trajectory, and its magnitude by the pulse size in the counter experiments and by the grain density in photographic emulsions. Ruling out the possibility of fractional charges, it is $-e$, identical with the charge of the electron (39).

Mass (14, 33, 39).—The first antiproton experiment gave the mass to an accuracy of 5 per cent. The most precise value of the ratio of the antiproton mass to that of the proton is obtained by the combined use of a measurement of momentum by the wire method and range in a photographic emulsion: a value of 1.010 ± 0.006 has been obtained for the ratio; however, the error reported does not take into account possible systematic errors in the determination of the momentum which, estimated very conservatively, might cause an error in the mass of about 3 per cent.

It is interesting to measure the mass of the antiproton by the use of photographic emulsions only, without a separate measurement of the momentum: this has been accomplished by (*a*) the combination of ionization and residual range and (*b*) by the combination of ionization and multiple scattering. Ionization was measured by grain density or by measuring the average fraction of a track occupied by silver grains. The emulsions were calibrated directly, using protons or deuterons. This work has given a ratio for Method (*a*) of 1.009 ± 0.027, and for Method (*b*) of 0.999 ± 0.043. Again the errors are only statistical. Possible systematic errors might be as high as 3 per cent (14).

The conclusion is that the identity of the mass of the proton and of the antiproton has been verified experimentally to an accuracy of about 2 per cent.

Spin and magnetic moment.—There are no direct observations of these quantities for the antiproton. A possible method of measurement would be the following: antiprotons generated with a momentum vector at an angle with the momentum of the particle incident on the target are likely to be polarized. If so, the polarization is in a direction perpendicular to the plane defined by the two momenta mentioned above. If the antiprotons are not polarized at creation, they may be polarized by scattering but this would increase very appreciably the intensity requirements for an experiment. Assume they are polarized and pass them through a magnetic field H parallel to the momentum. The polarization vector rotates by an angle

$$2\frac{\mu H d}{\hbar c \beta} = \alpha \qquad 3.$$

where μ is the magnetic moment, d the length of the field, and $\hbar$ Planck's constant divided by 2π. The angle α is directly measurable by scattering the antiprotons on a target and observing the asymmetry of scattering at different azimuths. All other quantities except μ are easily measurable. The experiment seems feasible with present techniques (67, 97). The spin of the antiproton could also be considered as directly verified experimentally if the magnetic moment were to be found, as expected, equal in magnitude to that of the proton; in fact, the factor 2 of Equation 3 is based on a spin $\frac{1}{2}$ for the antiproton; however, strictly speaking, this experiment would measure only the gyromagnetic ratio of the antiproton.

Annihilation.—The prediction from Table I is that a nucleon-antinucleon pair at rest will annihilate, releasing the energy $2\ mc^2$. No information is given on the form of the energy release; thus, for an electron-positron pair, γ-rays are emitted, whereas for a nucleon-antinucleon pair, pion production is the dominant mode of annihilation. Starting from a nucleon-antinucleon pair, positive, negative, or neutral pions may be obtained, the latter decaying within 10^{-15} sec. into γ-rays. The charged pions also decay into μ mesons and neutrinos, but the μ mesons decay further into electrons, positrons, and neutrinos; and in matter the positrons left over annihilate with electrons. Thus, within microseconds the whole rest mass of the system has degraded to forms of energy of rest mass zero with the exception of the case of the antiproton-neutron annihilation, in which an electron is left over. Without entering, at present, into any details concerning the annihilation process, it is clear that in a photographic emulsion where only charged particles leave a track it will not be possible to follow all the annihilation products, but only the charged ones. If, however, at the stopping point of an antiproton an energy release greater than mc^2 is observed, the conclusion must be drawn that the antiproton has annihilated another nucleon, because the visible energy liberated is already greater than the rest energy of the antiproton. The first observation of this phenomenon is reported in (32).

Other methods of observing the annihilation of an antiproton are based on the light emitted either as Cerenkov light or as scintillation light by the charged particles produced directly or indirectly in the annihilation process.

Two typical instruments using Cerenkov light and scintillation light, respectively, are shown in Figures 2 and 3. In Figure 2 the radiator is a large block of glass of refractive index 1.649 for the D lines and radiation length of 2.77 cm. It is observed by a bank of photomultipliers. The light observed is Cerenkov radiation due to the showers produced by neutral pions or produced directly by charged pions (23). In Figure 3 (30) the radiator is a composite sandwich of lead and plastic with an average density of 3.84 gm. cm.$^{-3}$, an average radiation length of 1.7 cm., and a thickness corresponding to three annihilation mean free paths. The total dimensions of the "sandwich" are about $60\times60\times60$ cm. Both instruments have low resolving power, and the annihilation of an antinucleon produces pulses which vary greatly in magnitude. Nevertheless, an apparatus similar to that of Figure

2 was used in order to see large annihilation pulses when antiprotons selected by the spectrograph of (39) were sent into a piece of glass. The results obtained "were not inconsistent with the expected behavior of antiprotons," but the largest energy release observed as Cerenkov light corresponded only to 0.9 Bev (21, 22).

Production in pairs.—The evidence on this subject comes from the excitation function. The data are still very scanty, but the fact that no anti-

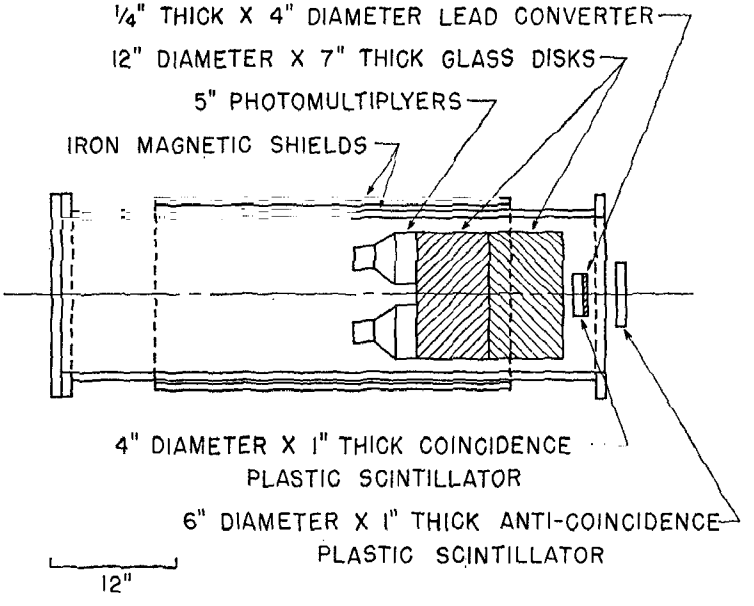

FIG. 2. Schematic arrangement of the pulse height spectrometer showing the glass phototubes, and magnetic shield, as well as the anticoincidence counter, lead, and coincidence counters. These two scintillation counters insure that the electron showers, which are pulse height analyzed, start in the 0.25-inch lead converter and thus are centered in the glass, and start at its front surface. From (23).

protons have been observed at an energy lower than 4.0 Bev for the Bevatron beam is an indication of the production in pairs (39).

Thresholds for production in pairs are given in the following Table III for different processes. Very little is known of the production cross sections and their energy-dependence (see section on Production), but if the production were not in pairs, process (1) with protons at rest would have, for instance, a threshold of only 2.35 Bev and the other correspondingly lower. The observed facts do not seem reconcilable with such an hypothesis:

Decay constant.—Antiprotons in a vacuum must be stable. Antineutrons must decay with a mean life of 1040 sec. In the different experiments per-

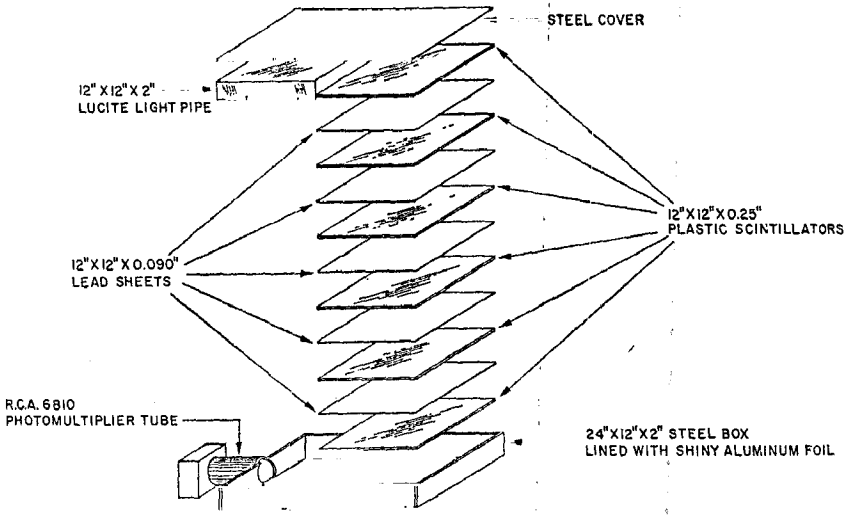

FIG. 3a. Element of the annihilation detector. From (30).

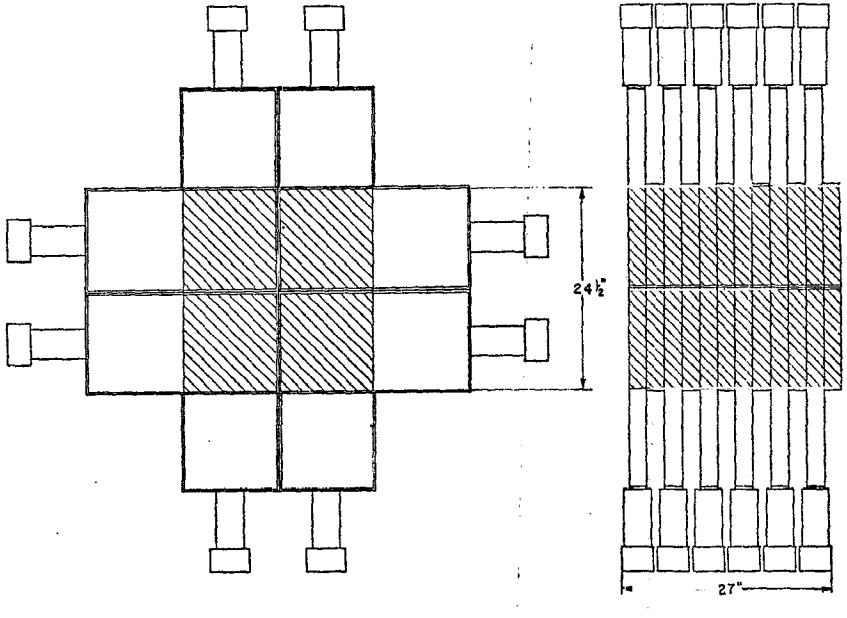

FIG. 3b. Assembly of the annihilation detector. From (30).

TABLE III

THRESHOLDS FOR NUCLEON ANTINUCLEON PAIR-PRODUCTION
(Bev kinetic energy in the laboratory)

Process	Target at rest	Target with Fermi Energy of 25 Mev
1) $p+p\rightarrow 3p+\bar{p}$	5.63	4.30
2) $\pi+p\rightarrow 2p+\bar{p}$	3.60	2.85
3)* $p+p\rightarrow p+p+\pi$	($T_\pi=3.60$) 4.06	($T_\pi=2.85$) 3.08

p stands for proton or neutron. Naturally electric charge must balance in the reaction.

* Line 3 indicates the proton minimum energy required in order to obtain pions of energy T_π in a p-p collision.

formed heretofore, the times of flight involved are up to 10^{-7} sec. The decay constant cannot be much less than the time of flight, otherwise no antiprotons would be observed. Thus the lower limit for the mean life is 10^{-7} sec.

In conclusion it can be said that the properties of Table I are essentially verified.

NUCLEONIC PROPERTIES OF THE ANTIPROTON

The total isotopic spin T of an antinucleon is clearly 1/2 and the formula for the charge

$$\frac{q}{e}=T_3+\frac{N}{2} \qquad 4.$$

where N is the number of nucleons, suggests the assignment of $T_3=-\frac{1}{2}$ to the antiproton and $T_3=\frac{1}{2}$ to the antineutron. Thus a proton-antiproton pair has $T_3=0$, but $T=1$ or 0, whereas the proton-antineutron pair or the antiproton-neutron pair have $T=1$.

The intrinsic parity of the antiproton and the antineutron is -1 if that of the proton and neutron is assumed to be $+1$. A justification of this assignment of intrinsic parity is that Dirac's theory predicts for the electron-positron pair in the $^1S_0$ state a 2-quanta annihilation with the polarization of the 2 quanta perpendicular to each other corresponding to a pseudoscalar matrix element $(\boldsymbol{e}_1\cdot\boldsymbol{e}_2\times\boldsymbol{p})f(p)$ ($\boldsymbol{e}_1$, $\boldsymbol{e}_2$ unit vectors indicating the polarization of the quanta; $\boldsymbol{p}$ relative momentum). This prediction has been verified experimentally and forces the electron and positron to have opposite parities [see (44)]. The same is assumed to hold for the proton-antiproton pair and for the neutron-antineutron pair. A summary of these properties is presented in Table IV (83, 90, 105).

The next discussion will be on those properties which are not predictable on the basis of charge conjugation. They are the most novel ones and their study has barely begun. They will be divided into collision cross sections, modes of annihilation, and production.

TABLE IV

SPIN, PARITY, *I*-SPIN OF NUCELONS AND ANTINUCLEONS

	Proton	Neutron	Antiproton	Antineutron
Spin S	1/2	1/2	1/2	1/2
I-spin T	1/2	1/2	1/2	1/2
3rd comp. of I-spin T_3	1/2	−1/2	−1/2	1/2
Parity	+	+	−	−

Collision cross sections.—Collisions of antiprotons on nuclei may lead to elastic scattering, inelastic scattering, annihilation, or charge exchange. The corresponding cross sections will be called σ_e, σ_i, σ_a, σ_c. Also considered is the reaction cross section $\sigma_r=\sigma_i+\sigma_a+\sigma_c$ and the total cross section $\sigma_t=\sigma_r+\sigma_e$. The experimental data obtained thus far are rather sketchy. The case of antiproton-nucleon scattering and the case of scattering from complex nuclei will be treated separately.

A typical apparatus used experimentally (36) is shown in Figure 4. A certified antiproton falls on the target which is placed in the slots of Y and, if it is annihilated, it gives Cerenkov light detectable by the photomultipliers. If it crosses the target without annihilation and falls into a cone of semi-aperture 14° or 20° it is detected by the circular scintillators. If it is scattered by an angle $\theta \geq 20°$ it is not detected by the scintillators or by the target box.

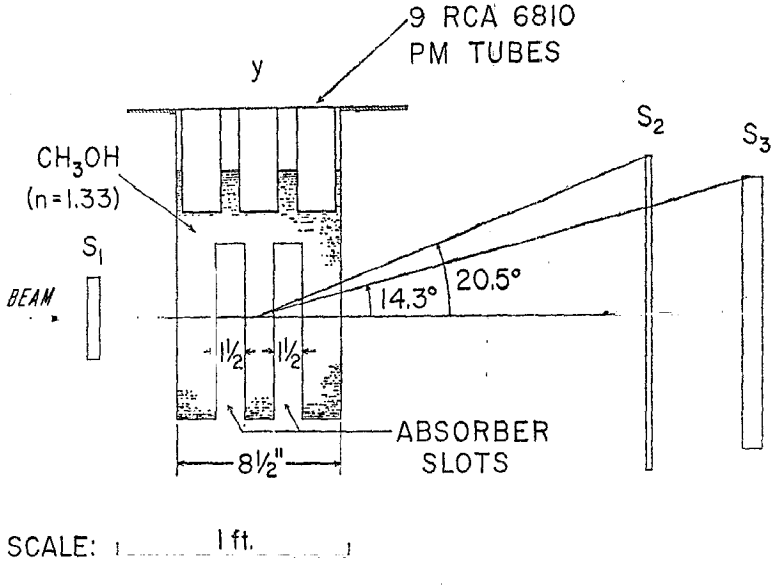

FIG. 4. Arrangement for measuring annihilation cross section and $\sigma_t(\theta)$. From (36).

With this apparatus one measures separately σ_a and σ_e (20°); the latter symbol means that the elastic scattering has occurred with an angle larger than 20°. A "good geometry" arrangement which measures σ_t is shown in Figure 5 (43). The data accumulated with these or other methods are shown in Tables V and VI. The errors quoted are only statistical. The whole subject is in a very early stage of development and the picture we have thus far is a sketchy one. Moreover, there are some features of the experimental results obtained thus far which look suspicious; in particular, the ratio between the scattering and total cross section in hydrogen should be reinvestigated.

It must be noted that most of the diffraction scattering is included in the data for beryllium and carbon. Namely, if one computes $\sigma_e(\theta)$ for $\theta = 0$, in-

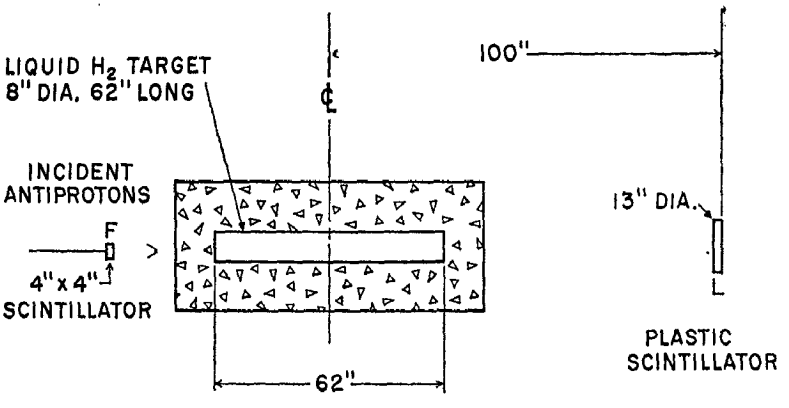

FIG. 5. Good geometry arrangement for measuring total $\bar{p} - p$ cross sections. From (43).

cluding all diffraction, the cross sections are increased by about 10 per cent. In the data for oxygen, copper, silver, and lead, diffraction scattering is practically excluded because $\theta \geq 14°$.

In Table V the data at 450 Mev have been obtained by investigation of H_2O, D_2O, and liquid oxygen and by suitable subtraction procedures. The reason for this is that liquid hydrogen has a refractive index too small to be used in a Cerenkov counter to detect annihilation. The data "n" are a simple subtraction of D_2O and H_2O observations. However, a large "Glauber correction" (58) is necessary in order to take into account the shielding of the neutron by the proton in the deuteron. The extent of this correction is somewhat uncertain (20, 58). The data n are corrected values.

The data on hydrogen give the puzzling result that if the data in good geometry are compared with the data at 450 Mev which are in poor geometry, there is no difference in cross section to account for any diffraction scattering. This point needs further experimental investigation.

The salient fact emerging from all these observations is that the cross sections which are obtained for all processes involving antiprotons are large

(37). There have been many theoretical papers on the interpretation of the $\bar{p}$ cross sections. At present the most promising line of approach to the interpretation of the experimental results seems to be a theory of Ball & Chew [12; see also 69, 73, 108] which accounts for the large $p\bar{p}$ and $n\bar{p}$ cross sections. Combination of their nucleon-antinucleon results with the optical model theory will account for the antiproton cross sections in complex nuclei.

TABLE V

ANTIPROTON NUCLEON CROSS SECTIONS (IN MILLIBARNS)

	T Mev	θ degrees	$\sigma_e(\theta)$	σ_a	σ_c	$\sigma_t(\theta)$‡	σ_t proton*†	σ_t neutron*†	Reference
H	20–230	5	71±25	≲86±45					60
	150	0	58±11						3
	133	0	72±10		10±3	166±8	28	54	41
	190	0				135±16	25	45	41
	197	0	64±8		11±3	152±7	25	44	41
	265	0	50±7		8_{-3}^{+6}	124±7	24	37	41
	300	0				104±14	23	35	43
	333	0	49±5		7±2	114±4	23	34	41
	450	14	15±12	89±7	10±6	104±8	(25)	33	36
	450	20	17±12			102±8	(24)	33	36
	500	0				97±4	30	35	43
	700	0				94±4	45	35	43
D	450	14		135±7		174±8	(54±2)	—	36
	450	20				172±8	(45±2)	—	36
"*n*"	450	14		46±8		70±8	(29±1)		36
	450	20				70±8	(21±1)		36
n	450	14		74		113			36
	450	20		74		113			36

* From the compilations of Beretta, L., Villi, C., and Ferrari, F., *Nuovo cimento*, **12**, Suppl., 499 (1954); Djelepov, V. P., and Pontecorvo, B., *Atomnaya Energ.*, **3**, 413 (1957).

† Numbers in parenthesis directly measured [see (36)].

‡ $\sigma_t(\theta)=\sigma_a+\sigma_c+\sigma_e(\theta)+\sigma_i$; for $\theta=14°$ or larger most of the diffraction scattering is not counted in $\sigma_t(\theta)$.

The Ball-Chew model starts from an analogy with nucleon-nucleon scattering. There a model with a repulsive core of $(1/3)(\hbar/m_\pi c)$ radius and a pion cloud surrounding it is assumed and has been shown by Gartenhaus (54) and by Signell & Marshak (99) to give reasonably good agreement with experi-

TABLE VI

$\bar{p}$-COMPLEX NUCLEI CROSS SECTIONS (IN MILLIBARNS)

Target	T (Mev lab)	θ degrees	$\bar{p}$			p^+	$\sigma_r\bar{p}/\sigma_r p^+$	References
			$\sigma_r(\theta)$	σ_a	$\sigma_t(\theta)$	$\sigma_r(\theta)$		
Be	500	2.57			460			43
	500	0			484± 60			43
	700	3.65			367			43
	700	1.90			416			43
	700	0			425± 50			43
C	700	25.0	436± 19					43
	700	2.64			575± 59			43
	700	0			657± 79			43
	300	3.55	568±102		618±111			43
	300	0			655±130			43
O	457	14	556± 10	453± 9		292± 2		2
	457	20	517± 10			246± 2		2
	457	0	590± 12			340± 4	1.74±0.04	2
Cu	411	14	1240± 82	1040± 61		719± 5		2
	411	20	1220± 88			640± 4		2
	411	0	1260± 91			880±10	1.44±0.11	2
Ag	431	14	1630±170	1500±157		1052± 6		2
	431	20	1640±183			924± 6		2
	431	0	1635±188			1170±12	1.39±0.16	2
Pb	436	14	2850±225	2010±182		1662±36		2
	436	20	2680±254			1461±10		2
	436	0	3005±275			1845±40	1.62±0.16	2
	650		2330±285					43

ment. The nature of the hard, repulsive core is unaccounted for from a pion-theoretical point of view and must be considered as a phenomenological hypothesis, whereas the pion cloud can be treated from the point of view of the Yukawa interaction with due refinements. For a nucleon-antinucleon system the hard, repulsive core is replaced by an absorbing core. This is motivated by theory and justified by the large experimental annihilation cross section. Any antiproton which overlaps even slightly with the core seems to undergo annihilation. This core is surrounded by a meson cloud charge conjugate to the meson cloud surrounding a proton, and the interaction between proton and antiproton can be calculated by the same methods as the proton-proton cross section, provided one remembers that the "mesonic charge" of the antiproton and of the proton are opposite. Thus forces derived from the exchange of an even number of pions have the same sign in both cases, but forces derived from the exchange of an odd number of pions have opposite signs in the two cases. This program is carried out by introducing an interaction energy

$$V_c + V_{LS}(L\cdot S) + V_T S_{12} \qquad 5.$$

containing a central, spin-orbit, and tensor part. From this one obtains an "equivalent potential" for the eigenstates of the total angular momentum including centrifugal repulsion:

$$V\begin{Bmatrix} l = J+1 \\ l = J-1 \end{Bmatrix} = V_C - \frac{3}{2}V_{LS} - V_T + \frac{J(J+1)+1}{Mr^2} \pm \left[\left(\frac{2J+1}{Mr^2} - \frac{2J+1}{2}V_{LS} - \frac{3V_T}{2J+1}\right)^2 + \frac{36J(J+1)}{(2J+1)^2}V_T^2\right]^{1/2} \quad 6.$$

$$V(l = J) = V_C - V_{LS} + 2V_T + \frac{J(J+1)}{Mr^2} \quad 7.$$

With these potentials one constructs the phase shifts and the penetration coefficients for the partial waves.

The V_C, V_{LS}, V_T are chosen following Gartenhaus (54) and Signell & Marshak (99) for the V_{LS} part, but introducing the sign changes required by the change of sign of the interaction energy corresponding to the exchange of one pion. The calculation of Ball and Chew is limited to s, p, and d waves, i.e., to energies <150 Mev, but even so it gives very interesting results as shown in Table VII.

TABLE VII

THEORETICAL CROSS SECTIONS FOR NUCLEON ANTINUCLEON INTERACTION IN MB AT 140 MEV (LAB) ACCORDING TO (30)

	$p\bar{p}$	$n\bar{p}$	pp	np
Absorption	73	69		
Scattering	74	79	29	60
Charge exchange	21			

The limitation in energy of the present calculations derives first from the nonrelativistic approximations made, as for instance the use of a potential; and second from the fact that in order to extend the theory to higher energies details near the boundaries of the black zone, which are unknown, become important. The reason for this is that the total potential surrounding the core is composed of a centrifugal part and a part originating from the nuclear forces. The sum of the two forms a barrier which is very wide and flat on the top. This barrier can be treated very adequately with the WKB method and for a given s, p, or d partial wave usually gives either perfect transparency or perfect opacity, fairly independently of any reasonable core radius. For higher angular momenta these circumstances no longer obtain.

The Ball-Chew model also can be used to calculate angular distributions for elastic scattering. These have been computed by Fulco (53) and show a peak in the forward direction (Fig. 6), very different from the np angular distribution. Experimental results, although not very abundant yet, seem to confirm this feature of the model, which is mainly due to the diffraction scattering connected with the annihilation (3). It is necessary to check further the prediction of this type of model against experiment, but at this time it seems to offer great promise of accounting for the facts.

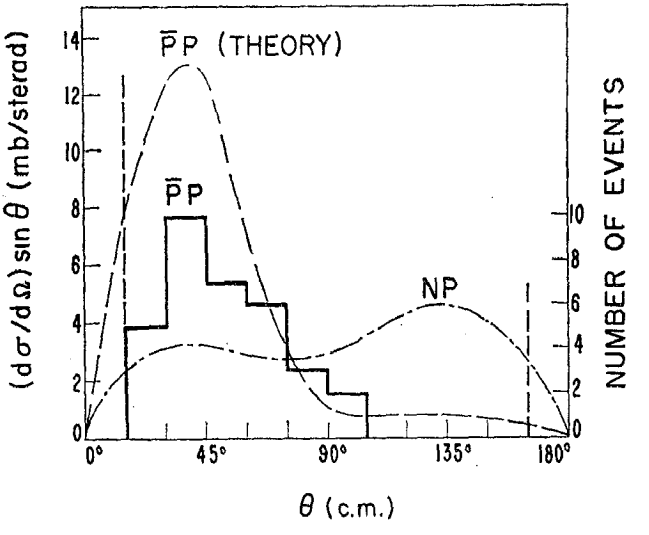

FIG. 6. Angular distribution in $p\bar{p}$-scattering. Theoretical curve from (53) at 140 Mev. Experimental results from (3).

In the same trend of ideas Koba & Takeda (73) conclude that at very large energies ($\lambda\!\!\!^{-} \ll a$), $\sigma_a = \sigma_e = \pi a^2$ where a is the radius of the black core, but at lower energies $\sigma_a = \pi(a+\lambda\!\!\!^{-})^2$. Even considering waves of high angular momentum l, the ratio between annihilation and scattering cross sections is limited by the inequality:

$$\sigma_t^{(l)} \leq \frac{4\pi}{k^2}(2l+1)\,\frac{\sigma_e^{(l)}}{\sigma_t^{(l)}} \qquad 8.$$

where $\sigma^{(l)}$ is the cross section for the lth partial wave. Thus, for a given total cross section, a small ratio of elastic to total cross section can be obtained only for large values of l.

Other calculations on the same subject have been performed by Lévy (80). In some respects these resemble Ball and Chew's work, but they try to take into account terms in which many pions, not only one or two, are involved [see also (102)]. They have been further developed by Gourdin *et al.* (64).

Inelastic collisions in which pions are generated, without annihilation of the antinucleon, have been considered by Barshay (15). He has established selection rules and angular distributions to be expected in such collisions.

In addition to the detailed considerations discussed above there are several relations between elastic cross sections which are independent of detailed models and require only charge independence of nuclear forces; such are found in (9, 31, 74, 83, 94). As examples we mention:

$$\frac{d\sigma}{d\omega}(0^0)_{p\bar{p}\to n\bar{n}} \geq \left(\frac{k}{4\pi}\right)^2 \{\sigma_t(\bar{p}n) - \sigma_t(p\bar{p})\}^2 \qquad 9.$$

where $\sigma_{p\bar{p}\to p\bar{n}}$ means the charge exchange scattering cross section and:

$$\sigma_e(p\bar{p}\to p\bar{p}) + \sigma_c(p\bar{p}\to n\bar{n}) \geq \tfrac{1}{2}\sigma_e(\bar{p}n\to\bar{p}n) \quad 10.$$

$$\sigma_e(p\bar{p}\to p\bar{p}) = \tfrac{1}{4}\left|a_{if}^{(0)} + a_{if}^{(1)}\right|^2 = \sigma_e(n\bar{n}\to n\bar{n}) \quad 11.$$

$$\sigma_c(p\bar{p}\to n\bar{n}) = \tfrac{1}{4}\left|a_{if}^{(0)} - a_{if}^{(1)}\right|^2$$

$$\sigma_e(\bar{p}n\to\bar{p}n) = \left|a_{if}^{(1)}\right|^2 = \sigma_e(\bar{n}p - \bar{n}p)$$

where $a_{if}^{(1)}$ is the scattering amplitude for $T=1$ (triplet) between initial and final states and $a_{if}^{(0)}$ is the scattering amplitude for $T=0$ (singlet) between initial and final state.

Relations 11 give rise to triangular inequalities:

$$\left|(\sigma(p\bar{p}\to\bar{n}n))^{1/2} - (\sigma(\bar{p}n\to\bar{p}n))^{1/2}\right| \leq (\sigma(p\bar{p}\to p\bar{p}))^{1/2} \leq (\sigma(p\bar{p}\to n\bar{n}))^{1/2} + (\sigma(\bar{p}n\to\bar{p}n))^{1/2} \quad 12.$$

$$\left|(\sigma(p\bar{p}\to n\bar{n}))^{1/2} - (\sigma(p\bar{n}\to p\bar{n}))^{1/2}\right| \leq (\sigma(\bar{p}n\to\bar{p}n))^{1/2} \leq (\sigma(p\bar{n}\to n\bar{p}))^{1/2} + (\sigma(p\bar{p}\to p\bar{p}))^{1/2} \quad 13.$$

$$\left|(\sigma(\bar{p}n\to\bar{p}n))^{1/2} \to (\sigma(p\bar{p}\to p\bar{p}))^{1/2}\right| \leq (\sigma(p\bar{p}\to n\bar{n}))^{1/2} \leq (\sigma(p\bar{n}\to p\bar{n}))^{1/2} + (\sigma(p\bar{p}\to p\bar{p}))^{1/2}. \quad 14.$$

These relations are valid for the differential cross sections as well as for the total cross sections.

At present there are not enough data to evaluate the scattering amplitudes. Pomeranchuk (94) has pointed out that at high energies we might expect:

$$\left|a_{if}^{(1)} - a_{if}^{(0)}\right| \ll \left|a_{if}^{(1)}\right| \quad 15.$$

$$\left|a_{if}^{(1)} - a_{if}^{(0)}\right| \ll \left|a_{if}^{(0)}\right|. \quad 16.$$

These interesting inequalities are justified as follows: for each initial state i of definite angular momentum and isotopic spin the scattering matrix to a given final state f is subject to the sum rule

$$\sum_f \left|S_{fi}\right|^2 = 1. \quad 17.$$

The amplitudes for elastic scattering in $T=0$ or $T=1$ states are $a_{if}^{(0)} = (S_{ii}^{(0)} - 1)$ or $a_{if}^{(1)} = (S_{ii}^{(1)} - 1)$, whereas all other amplitudes are S_{fi} for $f \neq i$. At high energies the S_{fi} become small because there are many channels and the sum rule forces each individual S_{fi} to be small; however the elastic scattering amplitudes stay comparable to unity because they are equal to $S_{ii} - 1$. As a consequence the amplitudes for elastic scattering $a_{if}^{(1)}$ and $a_{if}^{(0)}$ each tend separately to -1, whereas their difference tends to zero.

Proceeding from the nucleon-nucleon to the nucleon-nucleus processes, an early paper by K. A. Johnson (70) using lowest order perturbation theory predicted elastic cross sections of the order of 0.1 geometric. Duerr, M. H. Johnson & Teller (47, 71), on the basis of a special nonlinear theory of nuclear forces, predicted a total cross section of the order of or larger than the geometrical one. This theory now seems untenable (46), but it foresaw the experimental results.

The most successful treatments of the nucleon-nucleus interactions have been obtained with the optical model (2, 57, 84, 91, 93). In its simplest form one gives to nuclear matter a density distribution using, for example, data from electron scattering. Moreover, nuclear matter has absorption and scattering coefficients which can be connected with the nucleon-antinucleon scattering and annihilation. With such a nuclear model, using geometrical optics, the scattering and absorption by a nucleus are calculated. For a uniform spherical density distribution of radius R the reaction cross section of the nucleus is given by a literal application of geometrical (110) optics as

$$\sigma_r = 2\pi \int_0^R (1 - e^{-2Ks})bdb = 2\pi \int_0^R (1 - e^{-2Ks})sds \qquad 18.$$

where $s^2 = R^2 - b^2$, b is the impact parameter with respect to the center of the nucleus, and the absorption coefficient K is given by

$$K = 3A\bar{\sigma}/4\pi R^3 \qquad 19.$$

with A the mass number and $\bar{\sigma}$ the average total nucleon-antinucleon cross section. A slight refinement of this approach takes into account the finite range of the interaction and the nuclear density distribution. The density distribution used is generally of the form

$$\rho(r) = \frac{\rho_0}{1 + \exp\left[(r - R)/a\right]}. \qquad 20.$$

The parameters have been chosen in (2) with the following values

$$R = r_0 A^{1/3} = 1.08 A^{1/3} \times 10^{-13} \text{ cm.}; \; a = 0.57 \times 10^{-13} \text{ cm.} \qquad 21.$$

The results show good agreement with experiment.

In a similar fashion one may assume a complex potential (57)

$$V(r) = \frac{V + iW}{1 + \exp\left[(r - R)/a\right]} \qquad 22.$$

and calculate the cross sections. Glassgold has obtained good agreement with the present experimental data taking a potential of this form and $a = 0.65 \times 10^{-13}$ cm., $R = 1.30\, A^{1/3} 10^{-13}$ cm. He has calculated explicitly three cases corresponding to protons and antiprotons as shown in Table VIII.

TABLE VIII

OPTICAL MODEL POTENTIALS

(57) (For all three cases the radius parameter is $r_0 = 1.30$ and the diffuseness $a = 0.65$ 10^{-13} cm.)

Projectile	V (Mev)	W (Mev)
p	− 15	−12.5
$\bar{p}$	− 15	−50
$\bar{p}'$	−528	−50

Calculations with a deep potential well ($\bar{p}'$) as required by the hypothesis of Duerr and Teller seem hardly compatible with the experimental results.

Elastic collisions with small deflections give rise to interesting interference phenomena between coulomb and nuclear scattering. These have been observed in photographic emulsions by G. Goldhaber & Sandweiss (61). They considered scattering down to a projected angle 1.5° and compared the result with that calculated from a black sphere of radius R and a coulomb field. The radius R was assumed to be $1.64\ A^{1/3}10^{-13}$ cm. and corresponds to the annihilation cross section. The agreement with experiment is good. Similar calculations performed with the potentials used by Glassgold also agree with experiment and give further support for his choice $\bar{p}$ of parameters as distinct from the choice $\bar{p}'$.

A more fundamental approach to the determination for the constants of the optical model potential is to connect them to the nucleon-nucleon potential as indicated by Riesenfeld & Watson (111). In the specific case of the antiprotons, the Ball-Chew nucleon antinucleon potential may be used. Some successful steps in that direction have been initiated (3).

The annihilation process.—Information concerning the annihilation process is derived mostly from annihilations in photographic emulsions and bubble chambers (3, 6, 14, 33, 34, 35, 52, 68). From the technical side the most important development for observing the annihilation in photographic emulsions has been the preparation of beams in which the ratio of antiprotons to undesired particles is increased from the value obtained by a simple selection of momentum and direction from the Bevatron target. Such improved beams will be called "purified." In an unpurified beam the ratio of pions to antiprotons is in the range between 5×10^5 to 5×10^4, depending on the momentum selected. In order to have the $\bar{p}$ tracks easily distinguishable from minimum tracks at the entrance of the stack, it is necessary to keep the momentum below about 700 Mev/c. At this momentum the $\pi/\bar{p}$ ratio is about 5×10^5. Increase of the momentum at the entrance is undesirable, not only for the reason given above, but also to keep the stack length manageable.

Efforts to purify the beam were made at an early date by Stork *et al.* (100) but had meager success because the large absorption cross section for antiprotons, unknown at the time, spoiled the performance of the apparatus.

Later a method was devised by which a beam of selected momentum is passed through beryllium absorbers, out of which the different particles emerge with different momenta. A second momentum selector refocuses the different masses in different spots. The antiprotons are accompanied by a background of about 5×10^4 spurious particles per antiproton, which is a gain of a factor 10 in the ratio of antiprotons to background for the momentum considered. Moreover, the background particles are almost entirely electrons and mu mesons coming from the pion decay, with only a few per cent pions left. They interact only weakly in the plates and are much less disturbing than the original pion background (35).

The problem of purification of the beam is encountered also in the use

of bubble chambers. An arrangement (3) has been used in which a purification similar to the one described in (35) is combined with an electronic command of the flashing of the lights of the bubble chamber, limiting it to the cases when an antiproton detector signals the entrance of an antiproton in the bubble chamber.

The purification problem has also been attacked by a combination of electric and magnetic fields in a Wien-type velocity filter. This velocity selector is used in conjunction with momentum analyzers to separate particles of different mass. There are at present two versions of these separators (41, 89) which show great promise.

The annihilations in which the antiproton reaches the end of its range and is at rest will be discussed first. Actually, with the present photographic technique this means that the kinetic energy of the antiproton is <10 Mev.

Up to now it has not been possible to recognize effectively the partner in the annihilation in photographic emulsions. A few stars have been observed with no nucleons and an even number of mesic prongs, which could be attributed to $p\bar{p}$ annihilation, but no certain assignment is yet possible. At this time approximately 220 annihilation stars have been observed and analyzed in photographic emulsions. There are also about 500 stars in propane (3) and 50 in hydrogen (68) but their analysis is incomplete as yet. One hundred and twenty-seven of the photographic emulsion annihilations occurred at rest and 93 annihilations occurred in flight. A typical star is shown in Figure 7.

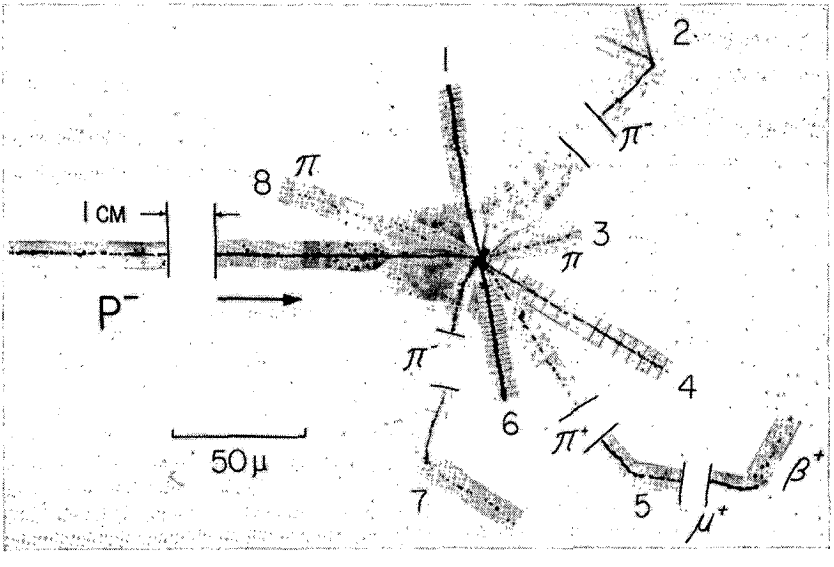

FIG. 7. An annihilation star (36) showing the particles as numbered.

No.	1	2	3	4	5	6	7	8
Identity	p?	π^-	π?	p	π^+	H^3(?)	π^-	π
T (Mev)	10	43	175	70	30	82	34	125

Total visible energy 1300 Mev. Total energy release >1400 Mev.

The fragments observed are π mesons, protons, light nuclei such as deuterons and α-particles, and sometimes, though rarely, K mesons. The maximum number of charged pions in a star thus far observed is six. The maximum number of charged nuclear particles thus far observed is 16. A distribution of the multiplicity of the charged pions is shown in Figure 8.

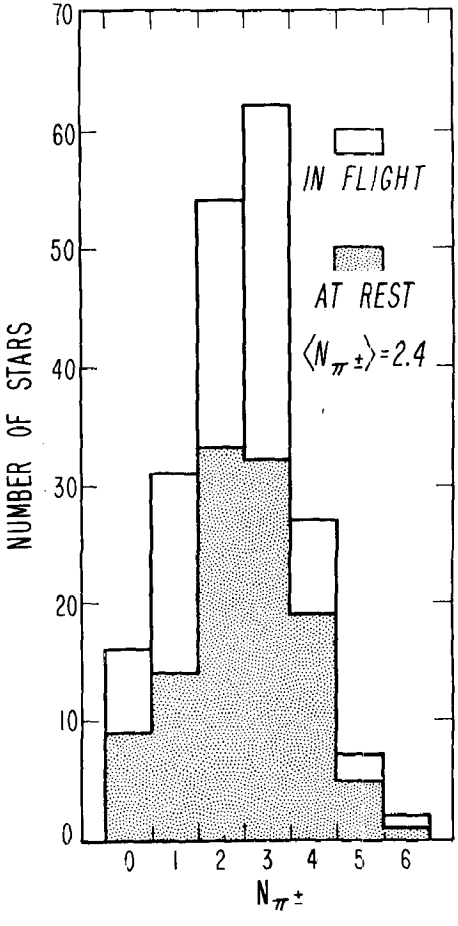

FIG. 8. Number of charged pions per annihilation star in photographic emulsions. Stars in flight give $\langle N_{\pi\pm}\rangle = 2.29 \pm 0.28$. Stars at rest give $\langle N_{\pi\pm}\rangle = 2.50 \pm 0.26$. These numbers are not corrected for scanning inefficiency (see text). From (35).

The following discussion is concerned with the experimental information on the visible energy release. The energy available is: $2\ mc^2 + T - B = W$, where T is the kinetic energy in the center of mass system and B the small (8 Mev) binding energy of the annihilating nucleon. In order to orient the reader on the apportioning of W, reference is made to Figures 10 and 11,

where the fraction of the visible energy going into pions, nucleons, or light nuclei is indicated. The few cases in which K mesons have been positively recognized are excluded from this figure.

Looking more in detail one finds a spectrum of pion energy as in Figure 9 with an average $T_\pi = 199 \pm 18$ Mev for charged pions. For the pions coming to rest in the stack ($T_\pi < 100$ Mev) it is also possible to determine the sign, and one finds a ratio of π^+ to π^- of 0.45 ± 0.1 (35). This number is smaller

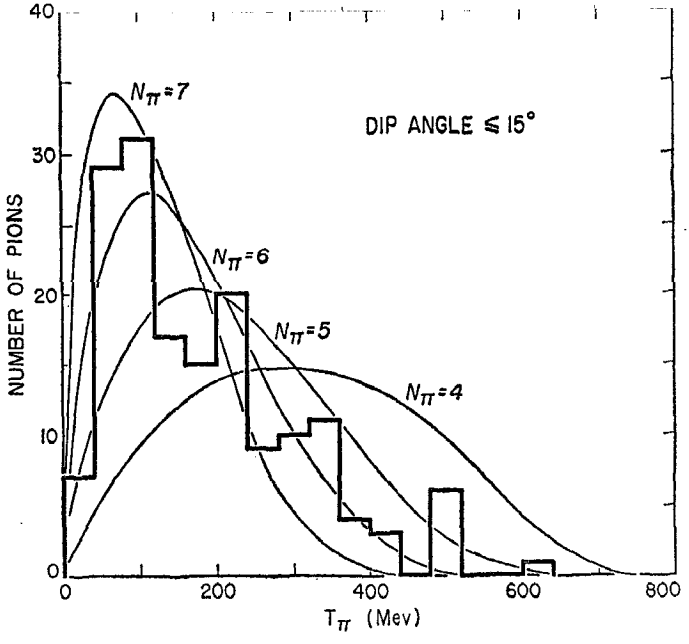

FIG. 9. Distribution of the observed kinetic energy of charged pions emitted in annihilation stars in nuclear emulsions. The curves marked $N_\pi = 4$, etc. are energy distributions obtained by the statistical method on the hypothesis that the average number of pions emitted is 4, 5, etc. Note that the experimental results agree with an average number of pions emitted lying between 6 and 7. From (35).

than one would expect on a naive view of the annihilation process which takes into account the n/p ratio in the nuclei and the conservation of isotopic spin (14, 92). It is, however, to be expected that this ratio is affected by the fact that the observations are limited to a low-energy region.

At this point one might try to estimate the ratio of the energy carried away by charged pions to that carried away by neutral pions. Figures 10 and 11 give a ratio of one to one for the energy carried away by all charged particles to that carried away by neutral particles. Neutrons in secondary processes are known to carry away about twice as much energy as charged nuclear fragments; moreover the efficiency for detecting charged pions is

estimated to about 0.9. Correcting for these factors the best estimate of the ratio of the energy carried away by charged pions to that carried away by neutral pions is 1.8.

It is now possible to calculate the average number of pions emitted per annihilation. The observed average charged pion multiplicity is 2.7 ± 0.2 pions per star. This figure contains a 10 per cent correction for scanning in-

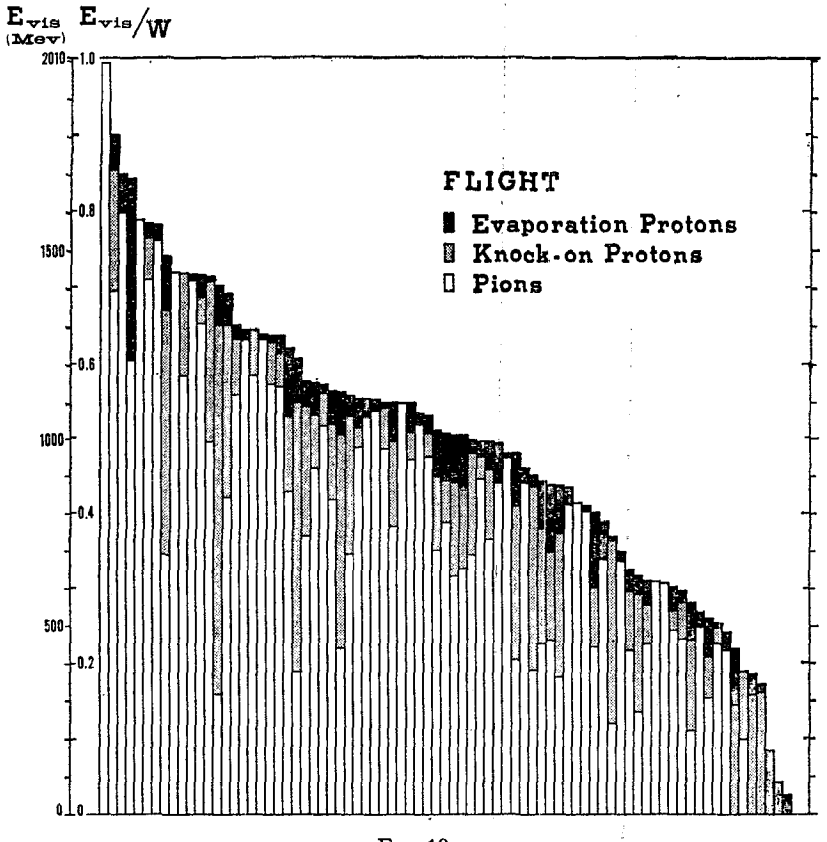

FIG. 10

(See Fig. 11 for caption.)

efficiency. Assuming that equal numbers of pions of each charge are produced in average in the annihilation process (see later), the number of pions emitted should be $3/2 \times (2.7 \pm 0.2)$ or 4.0 ± 0.3. To this number must be added the pions reabsorbed by the nucleus in which the annihilation occurred. Their energy is manifested by the nuclear fragments; they will be called "converted pions." The number of converted pions is approximately 1.3, as can be inferred from the fact that the nuclear fragments carry away an energy corresponding to 1.3 times the average total energy of a pion. In this estimate the energy carried away by the visible nuclear fragments is

multiplied by a factor 2.6 in order to take into account the energy carried by neutrons. By this method one thus arrives at an estimate of the average total number of pions released on annihilation, $\overline{N}_\pi$, of 5.3 ± 0.4.

A similar result also is reached if it is assumed that in annihilation the neutral pions have the same energy spectrum as the charged ones. Dividing the total energy available on annihilation by the average energy per pion (observed 338 Mev) one obtains 5.8 ± 0.3 for the number of pions. This is to

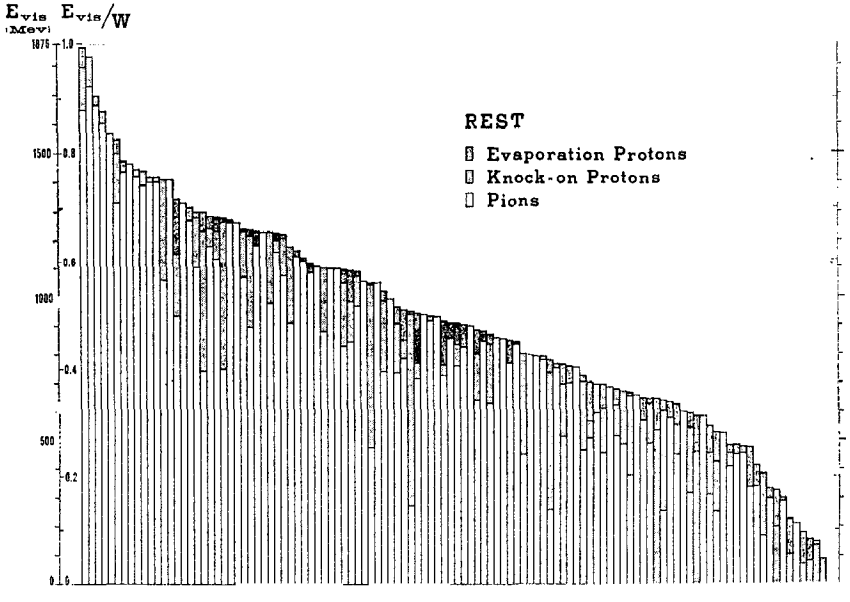

FIG. 11

FIG. 10 and 11. Visible energy in annihilation stars in photographic emulsions. Evaporation protons have $T < 30$ Mev by definition. Knock on protons have $T > 30$ Mev by definition. W is the total energy of the antiproton at annihilation. Note that stars in flight compared with stars at rest have a larger fraction of the energy in nucleons. From (35) and private communication.

be considered as an upper limit because the pions lose some energy before emerging from the nucleus and a better estimate is obtained by considering for each pion an average energy at formation of 360 Mev, and also the average energy going into K-mesons. With these corrections $\overline{N}_\pi = 5.3 \pm 0.5$.

The great majority of the annihilations in photographic emulsions occur in complex nuclei, and if the annihilation occurred deep inside the nucleus, the escaping pions would traverse the nucleus. The mean free path of pions of an energy of 180 Mev in nuclear matter is estimated to be about 10^{-13} cm. [see (81)], i.e., small compared with the nuclear radius, and the escaping pions would be "converted" into nucleons. The fact that only about one in

six of the pions is converted suggests that the annihilation occurs in the very peripheral parts of the nuclei and that most of the resulting pions escape without hitting the nucleus. The large nuclear cross sections are also evidence for this interpretation. Additional support for it comes from the observation that the number of pions "converted" in annihilations of antiprotons in flight is larger by about one than in the annihilations at rest as shown in Figures 10 and 11. This effect is interpreted as due to the deeper penetration of the antiproton in flight into the nucleus, compared to the antiproton at rest. An estimate of the order of magnitude of the mean life of the antiproton in nuclear matter, based on these considerations, is $\sim 2 \times 10^{-24}$ sec.

No angular correlations of the annihilation pions have been observed thus far, although one could perhaps expect that the nucleus should project a shadow and thus the pions might have a tendency to stay in a hemisphere. However, a pion-pion interaction might counterbalance this effect and a clarification of these questions will possibly come from the study of $\bar{p}$ annihilation in hydrogen where the shadow effect is obviously absent.

At the present time there are no separated examples of annihilations in different materials except for unanalyzed hydrogen stars. In propane some of the other stars are certainly due to carbon because they exhibit nucleons among their fragments, or have a balance of charge different from zero. Some might be due to $p\bar{p}$ annihilation but there is no proof that this is the case. For the stars produced by antiprotons coming to rest, there is a selective capture on the part of nuclei different from hydrogen similar to what occurs in the pion capture. The slowing down and capture of antiprotons are discussed theoretically by Bethe & Hamilton (19).

It is interesting to consider the possibility of "no prong" stars (95). They can be produced by charge exchange, in which the antiproton hits a proton and transforms into a neutron-antineutron pair, or by annihilation into neutral pions only. Both processes are rare and in photographic emulsions represent less than 1 per cent of the terminal events.

K-mesons have been found among the annihilation products in 3.5 ± 1.5 per cent of the photographic stars, and it is estimated that they carry away an average 50 ± 25 Mev per star. Λ-particles have also been found among the annihilation products.

On the theoretical side electromagnetic annihilation will be discussed briefly: it is similar to the electron positron (44) annihilation, but has not yet been observed. This is not surprising because it competes very unfavorably against the mesic annihilation. For instance, Brown & Peshkin (26) calculate for the annihilation in flight in the nonrelativistic limit a cross section

$$\sigma = \pi \left(\frac{e^2}{mc^2}\right)^2 \frac{c}{v} F(\lambda) \simeq 3.10^{-30} c/v \text{ cm.}^2 \qquad 23.$$

The factor $F(\lambda)$ takes into account the anomalous magnetic moment of the proton λ and has the numerical value 38.5. On the other hand, the mesic

annihilation cross section is of the order of 10^{-25} cm.^{2} The mixed annihilation, into γ-rays and mesons, is also very improbable. It has been considered by Michel (86).

For the purely mesic annihilation, the most important practically, many authors (1, 7, 8, 19, 56, 59, 69, 78) have established selection rules based on the conservation of angular momentum, parity, charge conjugation, and isotopic spin. It is possible to analyze the phenomenon with various degrees of detail. As an example, Table IX compiled by Lee and Yang and containing the main results is reproduced. In general, a given state can produce different numbers of pions; these numbers, however, are either all even or all odd. Thus, states of spin one produce only even numbers of pions. An interesting and exact consequence of charge independence concerns the average number of pions produced in annihilation of an antiproton on a proton and on a neutron, such as would be observed in annihilation against a nucleus containing the same number of neutrons and protons (55). We have then

$$\langle N(\pi^+)\rangle + \langle N(\pi^-)\rangle = 2\langle N(\pi^0)\rangle. \qquad 24.$$

Selection rules for the emission of K-particles on annihilation have also been considered by Goebel (59) and Gatto (56), and selection rules for the formation of pions in nonannihilating collisions of antiprotons and nuclei have been given by Barshay (15) as previously mentioned.

Apart from selection rules, repeated attempts have been made to apply Fermi's statistical theory (14, 17, 49, 101) to the nucleon-antinucleon annihilation. Using the theory in its simplest form, disregarding conservation of angular momentum and K-meson production, one obtains the results on the multiplicity of the mesons given in Table X.

The only arbitrary parameter entering in the calculation is the interaction volume Ω which is expressed in units of $(4/3\pi)(\hbar/m_\pi c)^3$. One would expect that the volume Ω should be near one, because the interaction range between nucleon and antinucleon is expected to be close to the pion Compton wavelength. The fact that agreement with experiment is obtained instead for Ω close to 10 needs some explanation. One of the most interesting and convincing ideas put forward is due to Koba & Takeda (73). They consider the nucleon and antinucleon surrounded by the pion cloud: on annihilation the bare nucleons destroy each other very swiftly, in a time of the order of $\hbar/2mc^2$, giving rise to a meson multiplicity corresponding to a value of Ω near one; but the mesons of the cloud at the moment of annihilation are also released, because the annihilation is a nonadiabatic process, with respect to the periods of the motions of the pions in the cloud which are of the order of $\hbar/E_\pi$ where E_π is the total energy of the pion in the cloud. E_π is estimated to be approximately 350 Mev from the energy of the annihilation pions. The number of pions in the cloud is estimated to be 1.3 per nucleon or antinucleon. In the annihilation 2.6 pions in average are interpreted as coming from the cloud, the remainder are interpreted as coming from the core annihilations. The core annihilation is treated by the statistical method,

TABLE IX

SELECTION RULES FOR $\bar{p}+p\rightarrow N\pi$ OR $\bar{q}+n\rightarrow N\pi$

State	Spin parity	C	T	G	$2\pi^0$	$\pi^+ +\pi^-$	$3\pi^0$	$\pi^+ +\pi^- +\pi^0$	$4\pi^0$	$\pi^+ +\pi^- +2\pi^0$	$2\pi^+ +2\pi^-$	$5\pi^0$	$\pi^+ +\pi^- +3\pi^0$	$2\pi^+ +2\pi^- +\pi^0$
$^1S_0$	0−	+	0	+	×	×	−	−				−	−	−
			1	−	×	×				−	−			
$^3S_1$	1−	−	0	−	×	−	×		×	−	−	×		
			−	+	×		×	−	×			×	−	−
$^1P_1$	1+	−	0	−	×	×	×		×	−	−	×		
			1	+	×	×	×	−	×			×	−	−
$^3P_0$	0+	+	0	+			×	×				−	−	−
			1	−	−	−	×	×	−	−	−			
$^3P_1$	1+	+	0	+	×	×	−	−				−	−	−
			1	−	×	×			−	−	−			
$^3P_2$	2+	+	0	+			−	−				−	−	−
			1	−	−	−			−	−	−			

× means strictly forbidden; − means forbidden so far as the isotopic spin is a good quantum number.

T = isotopic spin, C = charge conjugation operator, G is a quantum number of special interest in the case of systems of zero nucleons. It corresponds to the operator $C\,e^{i\pi T_2}$ and for zero nucleons has the eigenvalues ± 1 as indicated in the table.

TABLE IX—(*Continued*)

SELECTION RULES FOR $\bar{p}+n\rightarrow N\pi$

State	Spin parity	T	G	$\pi^- +\pi^0$	$2\pi^- +\pi^+$	$\pi^- +2\pi^0$	$2\pi^- +\pi^+ +\pi^0$	$\pi^- +3\pi^0$	$3\pi^- +2\pi^+$	$2\pi^- +\pi^+ +2\pi^0$	$\pi^- +4\pi^0$
$^1S_0$	0−	1	−	×			−	−			
$^3S_1$	1−	1	+		−	−			−	−	−
$^1P_2$	1+	1	+	×	−	−			−	−	−
$^3P_0$	0+	1	−	−	×	×	−	−			
$^3P_1$	1+	1	−	×			−	−			
$^3P_2$	2+	1	−	−			−	−			

× means strictly forbidden, and − means forbidden so far as the isotopic spin is a good quantum number.

TABLE Xa

DISTRIBUTION OF PION MULTIPLICITIES, ACCORDING TO FERMI MODEL, FOR DIFFERENT INTERACTION VOLUMES (PRODUCTION OF K MESONS NEGLECTED).

N_π	Probability for annihilation into N_π pions (%)		
	$\Omega=1$	$\Omega=10$	$\Omega=15$
2	6.4	0.1	0.0
3	63.7	5.6	2.3
4	24.6	21.7	13.4
5	5.0	44.0	40.6
6	0.3	23.7	33.1
7	0.0	5.1	10.6
Average No. of pions N_π	3.3	5.0	5.4

TABLE Xb

DISTRIBUTION OF PION AND K-MESON MULTIPLICITIES ACCORDING TO FERMI MODEL, FOR DIFFERENT INTERACTION VOLUMES

N_K	N_π	Probability for annihilation into N_π pions and N_K K mesons (%)		
		$\Omega=1$	$\Omega=10$	$\Omega=15$
0	2	3.8	0.0	0.0
	3	37.4	4.6	2.0
	4	14.5	17.9	11.8
	5	2.9	36.1	35.7
	6	0.2	19.5	28.9
	7	0.0	4.2	9.2
2	0	5.9	0.0	0.0
	1	26.7	3.3	1.4
	2	8.3	10.2	6.8
	3	0.3	4.1	4.1
	4	0.0	0.0	0.0
Average No. of pions N_π		2.4	4.5	5.0
Probability of producing a K-meson pair		41.2%	17.6%	12.3%

and using for the volume Ω the value 8/27, corresponding to a radius $(2/3)(\hbar/m_\pi c)$ consistent with other values used in the calculation of cross sections, one obtains 2.2 pions on the average from the core annihilation. Thus, the total average multiplicity would be 4.8, to be compared with the experimental value 5.3 ± 0.5. The hypothesis is developed further in order to obtain not only the average number of pions, but also the distribution among different multiplicities. Moreover, the number of K-mesons present in annihilation, which seems smaller than what is predicted by a straightforward application of the statistical theory, agrees better with the Koba-Takeda mechanism. Even if the quantitative agreement with experiment is not perfect, the reviewer thinks that this theory has considerable merit.

Other authors have stressed the many factors that could affect the annihilation process and are neglected in the statistical theory: such factors are the pion-pion interaction (63), the conservation of angular momentum, the relativistic conservation of the center of gravity (79), and other selection rules which might tend to suppress certain multiplicities. Indeed, it is apparent by considering the sensitivity of the results to some details of the calculation (17, 18) that the statistical method cannot reasonably be expected to give quantitative results, as was emphasized by Fermi himself. Adjustment of the parameter Ω might compensate for the crudeness of the approximation. Intermediate theories such as that of Heisenberg and Landau, or modifications of the original Fermi theory introducing a temperature parameter (75, 107), have also been tried with improved agreement with experiment. Conservation of the I-spin combined with the statistical theory also gives predictions for the $\pi^-:\pi^+:\pi^0$ ratio (92).

For the case of low multiplicities Bethe & Hamilton (19) have made a detailed analysis for capture in light elements, establishing in which states the capture must occur in order to give certain results. They consider also the "nuclear Auger effect." An antiproton is captured in a light nucleus from an atomic orbit and goes into a nuclear orbit releasing energy which is taken up by a nuclear proton that is ejected in a way similar to that of the Auger electrons in x-ray phenomena. It is doubtful that this effect takes place to any appreciable extent, since annihilation is probably much faster and takes place before the Auger jump.

An ingenious application of the K multiplicity to measure the spin of the K-meson has been made by Sandweiss (96). In the formulae for the K average multiplicity the statistical weight $(2I_K+1)$ of the K-meson appears and it should be possible to distinguish $I_K=0$ from $I_K=1$ or more. The average number of K-mesons per annihilation is very imperfectly known: the limits are from 1 to 4 per cent. In any case they point to spin 0 for the K-meson.

Production.—The collisions in which antiprotons are produced are most probably either of the type : $p+p \rightarrow 3p+\bar{p}$ or $\pi^-+p \rightarrow p+n+\bar{p}$, with all the variations compatible with charge conservation. In the observations up to now it is not known which of the two types of processes is most effective. Experimentally there are only very uncertain data: some measurements have

given 38×10^{-30} cm.^{2} ster.$^{-1}$ (Bev/c)$^{-1}$ per copper nucleus for the production in the forward direction at $\bar{p}$ momentum of 1.2 Bev/c when the target is bombarded with 6.1 Bev. protons (2).

A few comparisons between different targets show that for the same conditions protons are about as effective as carbon nuclei in producing antiprotons. Considering that the Fermi momentum should also enhance appreciably the production in carbon, the conclusion must be drawn that the nucleons in the carbon nucleus are very ineffective in giving antiprotons. The most natural explanation is the great absorption probability for antiprotons formed inside of the nucleus.

Some calculations which take into account mainly phase-space factors in the p-nucleus collision giving rise to antinucleons are reported in (49) and give $\sigma=0.6\times10^{-26}(\epsilon/mc^2)^{7/2}$ cm.^{2} Near threshold the yield of antiprotons should grow as $\epsilon^{7/2}$, where ϵ is the center-of-mass energy above threshold, if they are formed by pn collisions, or as $\epsilon^{9/2}$ if they are formed by pp collision. The extra factor ϵ in this case comes from the necessity of putting one of the outgoing protons in a p state.

Attempts have been made to derive production cross sections near threshold from pion theory: Thorn (104) has for the reactions: (*a*) $p+p\rightarrow\bar{p}+3p$ a cross section $1.4\times10^{-29}(f^2/4\pi)^4(\epsilon/mc^2)^{9/2}$ cm.^{2}, and for (*b*) $p+n\rightarrow n+2p+\bar{p}$ a cross section $5.4\times10^{-29}(f^2/4\pi)^4(\epsilon/mc^2)^{7/2}$ cm.^{2} with $f^2/4\pi=15$. Similar calculations by Fox (50) and McConnell (85) are based on an unlikely coupling. Calculations of some features of the production such as energy and angular distribution based on phase space considerations only are to be found in (33).

More recently Barasenkov *et al.* (13) have treated the antinucleon production problem by the statistical method following the idea of Belenky which considers a virtual particle corresponding to a pion and nucleon in the $J=3/2$ $T=3/2$ state. They also introduce two Fermi volumes corresponding to the Compton wavelength of the pion or of the K-meson, and they assume that the volumes to be considered in production differ for various particles. With these hypotheses they compute probabilities of formation of groups of particles and antiparticles at 7 and 10 Bev.

At extremely high energies ($>10^{13}$ev) the statistical method predicts the formation of $0.38(W'/mc^2)^{1/4}$ antiprotons in a nucleon-nucleon collision (W' laboratory energy of incident nucleon) (49).

Antineutrons.—The most convenient and up to now the only practical way of observing antineutrons is to obtain them from antiprotons by charge exchange and detect them by annihilation. This method of production was indicated immediately after the discovery of the antiproton (38) and first demonstrated experimentally by Cork, Lambertson, Piccioni & Wenzel (42) by a counter method in which an antiproton selected from a beam entered an absorber. No charged particle was seen to emerge from it, but an annihilation counter of the type described above showed an annihilation pulse. Similar experiments are reported in (30). The phenomenon is shown graph-

ically in Figure 12, which was taken with a propane bubble chamber (3). The antiproton, recognizable by the curvature and grain density of its track, comes to a sudden end because it loses its charge to a proton giving

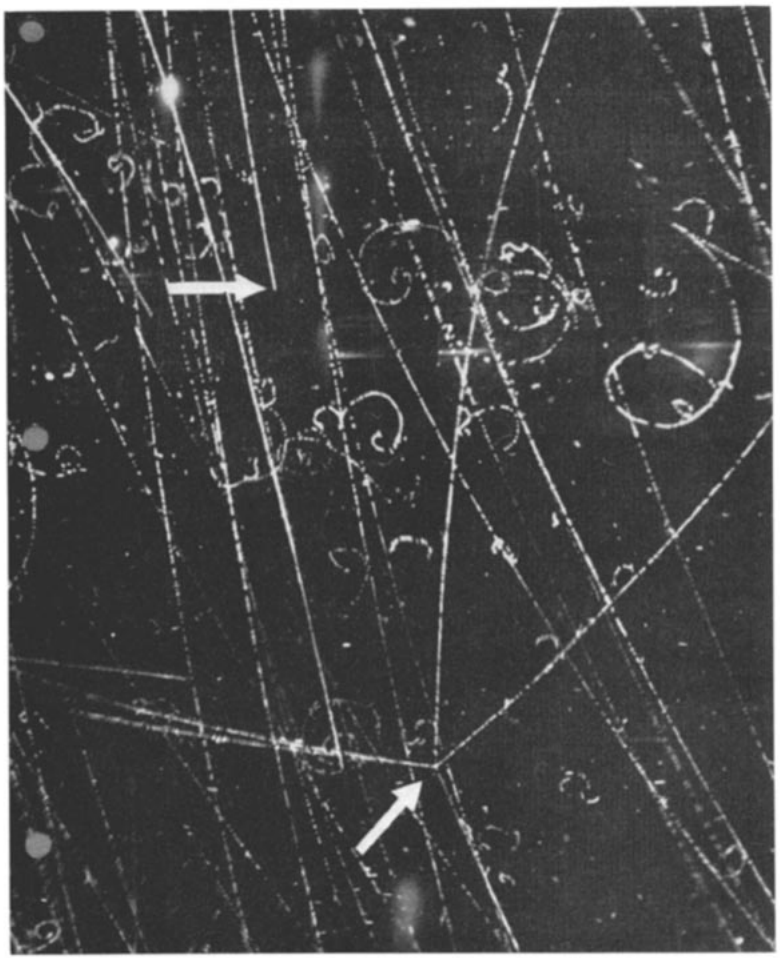

FIG. 12. An antiproton enters a propane bubble chamber, and at the point marked with the upper arrow undergoes charge exchange. The antineutron originates the annihilation star (lower arrow). Density of propane 0.42 gm. cm.$^{-3}$. Real distance between charge exchange and origin of star 9.5 cm. $T_{\bar{p}}$ at charge exchange $\sim$50 Mev. From (3).

rise to a neutron antineutron pair. The antineutron annihilates at the spot so marked, giving a typical annihilation star.

It would be highly desirable to be able to detect the antineutrons formed

at the target of the Bevatron without having to form first antiprotons and then charge exchange them. The primary difficulty is the problem of recognizing the antineutrons in the neutral beam emerging from the Bevatron. An ingenious attempt in that direction has been made by Moyer and his coworkers (109) in trying to use antineutrons formed in a reaction:

$$p + n = p + \bar{n} + p + n \qquad 25.$$

in which the three nucleons on the right escape combined as a He^3 nucleus. The reaction is thus a two-body reaction with kinematics such that detection of the He^3 at a certain angle from the incoming beam assures the presence of the $\bar{n}$ at another angle. Thus a coincidence system, possibly refined by time of flight measurements, should locate the antineutron uniquely. Unfortunately, here also the probability of the three nucleons forming a He^3 nucleus is low. There are not yet definite experimental results.

The charge exchange cross sections have been crudely measured and are indicated in Table V. Actually what has been measured is the integral of $(d\sigma/d\omega)_e$ in the forward directions for which $\theta \leq 17°$ (laboratory); for $p\bar{p}$ 10.9 ± 5.8 mb/ster. was obtained by (30). Most of the charge exchange will deliver antineutrons in a narrow cone in the forward direction in the laboratory, as in the np charge exchange. Explicit theoretical calculations based on the Ball-Chew model are given in (53).

The charge exchange for heavier nuclei has been also observed and there are indications (30) that at 500 Mev the charge exchange per nucleus does not vary greatly with A. This means, of course, that heavy nuclei are very inefficient as charge exchangers. Much of this result may be attributed to the large nucleon-antinucleon annihilation cross section which prevents the antiprotons from penetrating the nucleus, and gives rise to a shadow effect from the target. The antineutrons thus are only formed in grazing collisions with the rim of the target. If neutrons are concentrated on the surface of the nucleus, as is sometimes assumed, there is another reason for depressing charge exchange in heavy nuclei, because a $\bar{p}n$ collision may form antineutrons only if negative pions are emitted at the same time, a condition which certainly lowers the cross section.

Antihyperons.—There also must be antihyperons and the threshold for their formation by pion-nucleon collisions and nucleon-nucleon collisions in Bev (16) is indicated in Table XI.

Baldo-Ceolin & Prowse (11) have reported an event which might be interpreted as a $\bar{\Lambda}_0$ formed by a 4.5 Bev negative pion on a nucleus.

Antiprotons in cosmic rays.—A few possible antiprotons have been found in cosmic rays as mentioned above (6, 24, 25, 98, 103). A Bevatron event very similar in appearance to connected stars found in cosmic rays is reported in (65, 66).

Amaldi has commented on the frequency of observation of antiprotons in emulsions exposed to cosmic rays. His conclusion is that there are more antiprotons, perhaps by a factor 1000, in cosmic rays than one would expect

TABLE XI

Collision	$\bar{\Lambda}^0$	$\bar{\Sigma}$	$\bar{\Xi}$
nn	7.10	7.43	8.9
πn	4.73	5.24	6.12
Most favorable*	4.0	4.2	5.1

* Most favorable means a two stage reaction in which a pion is first formed (48) by a proton on a nucleus and Fermi energies are also considered.

from an estimate based on extrapolations of the Bevatron data (4). However, since the few examples known are doubtful the explanation of the difficulty might be simply found in the interpretation of the events.

Fradkin (51) has considered the possibility of the presence of antiprotons in the primary cosmic radiation and its effect on the east west asymmetry. He concludes that there are less than 0.17 per cent antiprotons in the primary radiation. McConnell (85) has also estimated the possible abundance of antiprotons in cosmic rays on the basis of meson theory. Nucleon antinucleon annihilation also has been invoked to explain the high-energy Schein events (85).

Cosmological Speculations

From the cosmological and astronomical point of view no direct telescopic observations can reveal antimatter. There are some unrealistic schemes, based on the helicity of neutrinos, which could in principle do it, but they are completely unfeasible at present.

Burbridge & Hoyle (27, 28) have calculated a maximum ratio of antimatter to matter for our galaxy of $\sim 10^{-7}$. They assume an average density of matter of 1 atom cm.$^{-3}$, and they show that the presence of antimatter in concentration larger than 10^{-7} atoms cm.$^{-3}$ would give rise to larger kinetic and magnetic energy of the interstellar gas clouds, and to cosmic radiation of greater intensity, than observed. They calculate also an upper limit for the possible rate of addition of antinucleons to our galaxy q, and find an upper limit of $q = 3 \times 10^{-22}$ antinucleons cm.$^{-3}$ sec.$^{-1}$. These would annihilate with a mean life of 3×10^{14} sec., and about 0.1 of the annihilation energy would go into electrons. The upper limit of q would obtain if the energy of the turbulent motions of the clouds could be ascribed entirely to these electrons.

The maximum value of q could be attained either by capture from an intergalactic medium or by a steady state production in an expanding universe. If the upper limit of the concentration of antimatter (10^{-7} nucleons cm.$^{-3}$) is reached, the radio noise of the Crab Nebula in our galaxy could be accounted for by the annihilation.

Outside of our galaxy the strong radio emission of Cygnus A and Messier 87 could also be due to annihilation processes. Burbridge & Hoyle (29) have pointed out some quantitative coincidences between the energy emitted and what could be expected on annihilation. One would then have a single ex-

planation for the energy of agitation of interstellar clouds in our galaxy, for the radio emission of the Crab Nebula, and for the two extragalactic sources Cygnus A and M 87.

In most cosmological speculations, both steady state and evolutionary, the conservation of nucleons and of leptons would require the simultaneous creation of matter and antimatter in equal amounts. This gives rise to the serious difficulty of a mechanism of separation of matter and antimatter, such as would be given by "antigravity." As an example of a cosmogonic speculation in which antimatter plays a prominent role the reviewer mentions the "universon" of M. Goldhaber (62).

The question of the gravitational behavior of antimatter can ultimately be resolved only by experiment. If the equivalence principle of general relativity is strictly valid, then the antiparticles are subject to the same gravitational actions as a particle of the same inertial mass. The inertial mass of the antiparticles is equal, also in sign, to that of the corresponding particles as shown by the method used for isolating them, which measures directly e/m, by the conservation of charge which establishes the sign of e, and by the laws of electromagnetism.

Even if we are willing to give up the equivalence principle and wish to speculate on "antigravity," namely, on the hypothesis that an antiparticle in a gravitational field be subject to the force opposite to that experienced by a particle, we meet a possible difficulty in the explanation of the behavior of a self-conjugate particle such as a photon, which is known to be subject to gravity.

The equivalence principle could be attributed to the fact that all masses in our universe (earth, sun, our galaxy) are composed of ordinary matter and that the equivalence principle is violated only to an extent connected to the concentration of antimatter in our universe (88). It is clear that all these arguments are extremely speculative and that the existence of antigravity would inflict severe damage on the present structure of physics. Also there is no really strong reason in its favor: on the other hand, only direct experiment can decide the question. For instance, it seems likely that an Eötvös-type experiment of slightly greater accuracy would show whether or not the virtual positrons that arise from vacuum polarization in the Coulomb field of the nucleus possess "antigravity" (96a).

LITERATURE CITED

1. Afrikian, L. M., *Soviet Phys. JETP*, **4**, 135 (1957)
2. Agnew, L. E., Chamberlain, O., Keller, D., Mermod, R., Rogers, E., Steiner, H., and Wiegand, C., *Phys. Rev.*, **108**, 1545 (1957)
3. Agnew, L. E., Elioff, T., Fowler, W. B., Gilly, L., Lander, R., Oswald, L., Powell, W., Segrè, E., Steiner, H., White, H., Wiegand, C., Ypsilantis, T., *Phys. Rev.*, **110**, 994 (1958); *Phys. Rev. Lett.* **1**, 27 (1958); (Private communication)
4. Amaldi, E., *CERN Symposium High-Energy Accelerators and Pion Phys. Geneva, Proc.*, **2**, 111 (1956)

5. Amaldi, E., Castagnoli, C., Cortini, G., Franzinetti, C., and Manfredini, A., *Nuovo cimento*, **1**, 492 (1955)
6. Amaldi, E., Castagnoli, C., Ferro-Luzzi, M., Franzinetti, C., and Manfredini, A., *Nuovo cimento*, **5** (10), 1797 (1957)
7. Amati, D., and Vitale, B., *Nuovo cimento*, **2**, 719 (1955)
8. Amati, D., and Vitale, B., *Nuovo cimento*, **3**, 1411 (1956)
9. Amati, D., and Vitale, B., *Nuovo cimento*, **4**, 145 (1956)
10. Anderson, C. D., *Phys. Rev.*, **43**, 491 (1933)
11. Baldo-Ceolin, M., and Prowse, D. J., *Bull. Am. Phys. Soc.*, **3**, 163 (1958)
12. Ball, J. S., and Chew, G. F., *Phys. Rev.*, **109**, 1385 (1958)
13. Barasenkov, V. S., Barasev, B. M., and Bubelev, E. G., *Nuovo cimento*, **7**, Suppl., 117 (1958)
14. Barkas, W. H., Birge, R. W., Chupp, W. W., Ekspong, A. G., Goldhaber, G., Goldhaber, S., Heckman, H. H., Perkins, D. H., Sandweiss, J., Segrè, E., Smith, F. M., Stork, D. H., Van Rossum, L., and Amaldi, E., Baroni, G., Castagnoli, C., Franzinetti, G., and Manfredini, A., *Phys. Rev.*, **105**, 1037 (1957)
15. Barshay, S., *Phys. Rev.*, **109**, 554 (1958)
16. Beasley, C. O., and Holladay, W., *Nuovo cimento*, **7**, Suppl., 77 (1958)
17. Belen'kii, S. Z., Maksimenko, V. M., Nikishov, A. I., and Rozental, I. L., *Uspekhi Fiz. Nauk*, **62**, 1 (1957)
18. Belen'kii, S. Z., and Rozental, I. L., *Soviet Phys. JETP*, **3**, 786 (1956)
19. Bethe, H., and Hamilton, J., *Nuovo cimento*, **4**, 1 (1956)
20. Blair, J. S., *Nuclear Phys.*, **6**, 348 (1958)
21. Brabant, J. M., Cork, B., Horwitz, N., Moyer, B. J., Murray, J. J., Wallace, R., and Wenzel, W. A., *Phys. Rev.*, **101**, 498 (1956)
22. Brabant, J. M., Cork, B., Horwitz, N., Moyer, B. J., Murray, J. J., Wallace, R., and Wenzel, W. A., *Phys. Rev.*, **102**, 1622 (1956)
23. Brabant, J. M., Moyer, B. J., and Wallace, R., *Rev. Sci. Instr.*, **28**, 421 (1957)
24. Bridge, H. S., Caldwell, D. O., Pal, Y., and Rossi, B., *Phys. Rev.*, **102**, 920 (1956)
25. Bridge, H. S., Courant, H., De Staebler, Jr., H., and Rossi, B., *Phys. Rev.*, **95**, 1101 (1954)
26. Brown, L. M., and Peshkin, M., *Phys. Rev.*, **103**, 751 (1956)
27. Burbridge, G. R., and Hoyle, F., *Astron. J.*, **62**, 9 (1957)
28. Burbridge, G. R., and Hoyle, F., *Nuovo cimento*, **4**, 558 (1956)
29. Burbridge, G. R., and Hoyle, F., *Sci. American*, **198**, 34 (1958)
30. Button, J., Elioff, T., Segrè, E., Steiner, H., Weingart, R., Wiegand, C., and Ypsilantis, T., *Phys. Rev.*, **108**, 1557 (1957)
31. Chamberlain, O., *Padova Venezia Conference, September, 1957* (In press)
32. Chamberlain, O., Chupp, W. W., Ekspong, A. G., Goldhaber, G., Goldhaber, S., Lofgren, E. J., Segrè, E., Wiegand, C., and Amaldi, E., Baroni, G., Castagnoli, C., Franzinetti, C., and Manfredini, A., *Phys. Rev.*, **102**, 921 (1956)
33. Chamberlain, O., Chupp, W. W., Goldhaber, G., Segrè, E., Wiegand, C., and Amaldi, E., Baroni, G., Castagnoli, C., Franzinetti, C., and Manfredini, A., *Nuovo cimento*, **3**, 447 (1956)
34. Chamberlain, O., Chupp, W. W., Goldhaber, G., Segrè, E., Wiegand, C., and Amaldi, E., Baroni, G., Castagnoli, C., Franzinetti, C., and Manfredini, A., *Phys. Rev.*, **101**, 909 (1956)
35. Chamberlain, O., Goldhaber, G., Jauneau, L., Kalogeropoulos, T., Segrè, E., and Silberberg, R., *Padova Venezia Conference* (Study of the annihilation process in a separated antiproton beam, in press)

36. Chamberlain, O., Keller, D. V., Mermod, R., Segrè, E., Steiner, H. M., and Ypsilantis, T., *Phys. Rev.*, **108**, 1553 (1957)
37. Chamberlain, O., Keller, D. V., Segrè, E., Steiner, H. M., Wiegand, C., and Ypsilantis, T., *Phys. Rev.*, **102**, 1637 (1956)
38. Chamberlain, O., Segrè, E., Wiegand, C., and Ypsilantis, T., *Nature*, **177**, 11 (1956)
39. Chamberlain, O., Segrè, E., Wiegand, C., Ypsilantis, T., *Phys. Rev.*, **100**, 947 (1955)
40. Chamberlain, O., Wiegand, C., *CERN Symposium High Energy Accelerators and Pion Phys., Geneva, Proc.*, **2**, 82 (1956)
41. Coombs, C., Cork, B., Galbraith, W., Lambertson, G. R., and Wenzel, W. A., *Bull. Am. Phys. Soc.*, **3**, 271 (1958); *Phys. Rev.* (In press)
42. Cork, B., Lambertson, G. R., Piccioni, O., and Wenzel, W. A., *Phys. Rev.*, **104**, 1193 (1956)
43. Cork, B., Lambertson, G. R., Piccioni, O., and Wenzel, W. A., *Phys. Rev.*, **107**, 248 (1957)
44. DeBenedetti, S., and Corben, H. C., *Ann. Rev. Nuclear Sci.*, **4**, 191 (1954)
45. Dirac, P. A. M., *The Principles of Quantum Mechanics* (Oxford University Press, London, Engl., 1st ed., 1930; 3rd ed., 1947)
46. Duerr, H. P., *Phys. Rev.*, **109**, 1347 (1958)
47. Duerr, H. P., and Teller, E., *Phys. Rev.*, **101**, 494 (1956)
48. Feldman, G., *Phys. Rev.*, **95**, 1697 (1954)
49. Fermi, E., *Progr. Theoret. Phys. (Kyoto)*, **5**, 570 (1950)
50. Fox, D., *Phys. Rev.*, **94**, 499 (1954)
51. Fradkin, M. I., *Soviet Phys. JETP*, **2**, 87 (1956)
52. Frye, G. M., and Armstrong, A. H., *Bull. Am. Phys. Soc.*, **3**, 163 (1958)
53. Fulco, J. R., *Phys. Rev.* **110**, 789 (1958)
54. Gartenhaus, S., *Phys. Rev.*, **107**, 291 (1957)
55. Gatto, R., *Nuovo cimento*, **3**, 468 (1956)
56. Gatto, R., *Nuovo cimento*, **4**, 526 (1956)
57. Glassgold, A. E., *Phys. Rev.*, **110**, 220 (1958)
58. Glauber, R. J., *Phys. Rev.*, **100**, 242 (1955)
59. Goebel, C., *Phys. Rev.*, **103**, 258 (1956)
60. Goldhaber, G., Kalogeropoulos, T., and Silberberg, R., *Phys. Rev.* **110**, 1474 (1958)
61. Goldhaber, G., and Sandweiss, J., *Phys. Rev.*, **110**, 1476 (1958)
62. Goldhaber, M., *Science*, **124**, 218 (1956)
63. Goto, T., *Soryushiron Kenkyu (Japan)*, **15**, 176 (1957); *Nuovo cimento*, **8**, 625 (1958)
64. Gourdin, M., Jancovici, B., and Verlet, L., *Nuovo cimento*, **8**, 485 (1958)
65. Hill, R. D., Johansson, S. D., and Gardner, F. T., *Phys. Rev.*, **101**, 907 (1956)
66. Hill, R. D., Johansson, S. D., and Gardner, F. T., *Phys. Rev.*, **103**, 250 (1956)
67. Hillman, P., Stafford, G. H., and Whitehead, C., *Nuovo cimento*, **4**, 67 (1956)
68. Horwitz, N., Miller, D., Murray, J. J., and Tripp, R., *Am. Phys. Soc.* (Washington meeting, 1958, post deadline paper)
69. Iwadare, J., and Hatano, S., *Prog. Theoret. Phys. (Kyoto)*, **15**, 185 (1956)
70. Johnson, K. A., *Phys. Rev.*, **96**, 1659 (1954)
71. Johnson, M. H., and Teller, E., *Phys. Rev.*, **98**, 783 (1955)
72. Koba, Z., *Progr. Theoret. Phys. (Kyoto)*, **19**, 594 (1958)
73. Koba, Z., and Takeda, G., *Progr. Theoret. Phys. (Kyoto)*, **19**, 269 (1958)

74. Kobsarev, I., and Schmuschkevic, I., *Doklady Akad. Nauk S.S.S.R.*, **102,** 929 (1955)
75. Kretzschmar, M., *Z. Physik*, **150,** 247 (1958)
76. Lee, T. D., Oehme, R., and Yang, C. N., *Phys. Rev.*, **106,** 340 (1957)
77. Lee, T. D., and Yang, C. N., *Elementary Particles and Weak Interactions* (Washington, D. C., 1957)
78. Lee, T. D., and Yang, C. N., *Nuovo cimento*, **3,** 749 (1956)
79. Lepore, J. V., and Neuman, M., *Phys. Rev.*, **98,** 1484 (1955)
80. Lévy, M., *Nuovo cimento*, **8,** 92 (1958)
81. Lindenbaum, S., *Ann. Rev. Nuclear Sci.*, **7,** 315 (1957)
82. Lüders, G., *Naturwissenschaften*, **43,** 121 (1956)
83. Malenka, B. J., and Primakoff, H., *Phys. Rev.*, **105,** 338 (1957)
84. McCarthy, I. E., *Nuclear Phys.*, **4,** 463 (1957)
85. McConnell, J., *Nuclear Phys.*, **1,** 202 (1956)
86. Michel, L., *Nuovo cimento*, **10,** 319 (1953)
87. Mitra, A. N., *Nuclear Phys.*, **1,** 571 (1956)
88. Morrison, P., *Am. J. Phys.* (In press)
89. Murray, J. J., *Bull. Am. Phys. Soc.*, **3,** 175 (1958)
90. Nakai, S., *Progr. Theoret. Phys.* (*Kyoto*), **17,** 139 (1957)
91. Nemirovskii, P. E., *Doklady Akad. Nauk U.S.S.R.*, **112,** 411 (1957)
92. Nikishov, A. I., *Soviet Phys. JETP*, **3,** 976 (1957)
93. Nozawa, M., Goto, T., Yajima, N., and Nakashima, R., *Progr. Theoret. Phys.* (*Kyoto*), **17,** 504 (1957)
94. Pomeranchuk, I. Ya., *Soviet Phys. JETP.*, **3,** 306 (1956); *Zhur. Eksptl. i Teoret. Fiz.*, **30,** 423 (1956)
95. Pontecorvo, B., *Soviet Phys. JEPT*, **3,** 966–(1957)
96. Sandweiss, J., *On the Spin of K-Mesons from the Analysis of Antiproton Annihilations in Nuclear Emulsions* (Doctoral thesis, AEC, Rad. Lab., W-7405-eng-48, 1956)
96a. Schiff, L. I. (Personal communication)
97. Segrè, E., *Padova, Venezia Conference* (In press)
98. Shrikantia, G. S., *Nuovo cimento*, **12,** 807 (1954)
99. Signell, P. S., and Marshak, R. E., *Phys. Rev.*, **109,** 1229 (1958)
100. Stork, D. H., Birge, R. W., Haddock, P. R., Kerth, L. T., Sandweiss, J., and Whitehead, M. N., *Phys. Rev.*, **105,** 729 (1957)
101. Sudarshan, G., *Phys. Rev.*, **103,** 777 (1956) (This paper contains numerical errors)
102. Tarasov, A., *Soviet Phys. JETP*, **3,** 636 (1956)
103. Teucher, M., Winzeler, H., and Lohrmann, E., *Nuovo cimento*, **3,** 228 (1956)
104. Thorn, R. N., *Phys. Rev.*, **94,** 501 (1954)
105. Wick, G. C., *Ann. Rev. Nuclear Sci.*, **8,** 1 (1958)
106. Wiegand, C., *Proc. I.R.E.*, (*Inst. Radio Engrs.*), *6th Scintillation Counter Symposium* (Washington, D. C., 1958)
107. Yajima, N., Kobayakawa, K., *Progr. Theoret. Phys.* (*Kyoto*), **19,** 192 (1958)
108. Yamaguchi, Y., *Progr. Theoret. Phys.* (*Kyoto*), **17,** 612 (1957)
109. Youtz, B., *Am. J. Phys.*, **26,** 202 (1958)
110. Fernbach, S., Serber, R., Taylor, T. B., *Phys. Rev.*, **75,** 1352 (1949)
111. Riesenfeld, W. B., and Watson, K. M., *Phys. Rev.*, **102,** 1157 (1956)

CONTENTS

PAGE

INVARIANCE PRINCIPLES OF NUCLEAR PHYSICS, *G. C. Wick* 1

THE OPTICAL MODEL AND ITS JUSTIFICATION, *Herman Feshbach* . . 49

HYPERFRAGMENTS, *W. F. Fry* 105

ANTINUCLEONS, *Emilio Segrè* 127

GAMMA-RAY SPECTROSCOPY BY DIRECT CRYSTAL DIFFRACTION, *Jesse W. M. DuMond* 163

CONCEPTUAL ADVANCES IN ACCELERATORS, *David L. Judd*. 181

THE PRIMARY COSMIC RADIATION, *H. V. Neher* 217

THE RADIOACTIVITY OF THE ATMOSPHERE AND HYDROSPHERE, *Hans E. Suess* 243

GEOCHRONOLOGY BY RADIOACTIVE DECAY, *L. T. Aldrich and G. W. Wetherill* 257

NUCLEAR ASTROPHYSICS, *A. G. W. Cameron* 299

PRACTICAL CONTROL OF RADIATION HAZARDS IN PHYSICS RESEARCH, *Burton J. Moyer* 327

CELLULAR RADIOBIOLOGY, *Thomas H. Wood* 343

INFORMATION THEORY IN RADIOBIOLOGY, *Henry Quastler* 387